This article has been accepted for publication in a future issue of this journal, but has not been fully edited. Content may change prior to final publication.
Citation information: DOI: 10.17775/CSEEJPES.2021.03330, CSEE Journal of Power and Energy Systems

Risk-constrained Energy Management Strategy for a Commercial Campus Considering Comprehensive Reserves Against Islanding Conditions

Zheming Liang, *Member, IEEE*, Desong Bian, *Member, IEEE*, Xiaohu Zhang, *Senior Member, IEEE*, and Di Shi, *Senior Member, IEEE*

***Abstract*—This paper proposes an optimal risk-constrained energy management strategy for commercial buildings in a commercial campus with islanding capabilities. The goal is to minimize the total operation and maintenance costs, while maximizing comprehensive comfort levels for the occupants. A two-stage risk-constrained, scenario-based stochastic optimization approach is adopted to handle various uncertainties associated with the energy management process, such as power generation of roof-top solar panels, arrival state-of-charges, and arrival/departure time of plug-in electric vehicles, intermittent load demand, and uncertain grid-connection conditions. A conditional-value-at-risk method is introduced to provide a risk-averse energy management strategy. To face the challenge of both reducing the computational burden and maintaining the accuracy of the stochastic programming, an advanced scenario reduction method is leveraged. Extensive simulation results validate the effectiveness of the proposed energy management strategy for minimizing the total operating and maintenance costs of commercial buildings with islanding capabilities, while maximizing the comprehensive comfort levels of the occupants.**

***Index Terms*—Comprehensive comfort levels, CVaR, Energy management, Islanding capability, Reserve, Stochastic programming, Uncertainty**

NOMENCLATURE

Sets and Indices

i	Commercial building (CB).
k	Plug-in electric vehicle (PEV).
t	Time slot.
j	Electric water heater (EWH).
n	Electrical storage (ES).
s	Scenario.
m	Renewable energy source (RES).
c	Combined heat and power (CHP).
N_i	Set of CBs.
N_k	Set of PEVs.
N_t	Set of time slots.
N_j	Set of EWHs.
N_n	Set of ESs.
N_s	Set of scenarios.
N_m	Set of RESs.
N_c	Set of CHPs.

This work is funded by State Grid Corporation of China (SGCC) under project "Hybrid Energy Storage Management Platform for Integrated Energy System" and contract number SGGR0000DLJS1800932.

The authors are with the GEIRI North America, San Jose, CA, USA. Zheming Liang is also with the Huaneng Renewables Co., Ltd. (e-mail: zheming_liang@hnr.com.cn).

Parameters

ϵ	Level of confidence.
κ	Level of risk aversion.
c_n	Degradation cost of ES n ($\$/kWh$).
c_p	Penalty for electricity exchange mismatch ($\$/kW$).
ζ_j/ζ_c	Power-to-heat ratio of EWH j/CHP c.
C_{water}	Water heat capacity ($J/(kg°C)$).
c_t^b	Price of natural gas ($\$/kBtu$).
$\overline{H}_j$	Maximum heating output of heat boiler j ($kBtu$).
L_j^s	Total energy consumed by EWH j (kJ).
M_j	Water mass in EWH j (kg).
D_t^s	Base power demand (kW).
Q_t^s	Base heat demand ($kBtu$).
t_j^a/t_j^d	Operation duration of EWH j (hr).
SU_c/SD_c	On/off cost of CHP c ($).
RU_c/RD_c	Ramping bounds of CHP c (kW).
UT_c/DT_c	Operation restriction periods of CHP c (hr).
$\overline{P}_c/\underline{P}_c$	Rated power generation of CHP c (kW).
β_c/γ_c	Cost parameters of CHP unit c ($\$/kW$).
$c_{\text{DA},t}^{s,+}$	Unit price of buying power from the day-ahead electricity market ($\$/kWh$).
$c_{\text{DA},t}^{s,-}$	Unit price of selling power to the day-ahead electricity market ($\$/kWh$).
$c_{\text{RT},t}^s$	Unit price of exchange power in the real-time ($\$/kWh$).
ρ_s	Probability of scenario s.
$w_{m,t}^s$	Power output of RES unit m (kW).
E_k^d	Desired energy level of PEV k (kWh).
η_k^+	Efficiency of charging PEV k.
P_k^+	Rated charging power of PEV k (kW).
$\underline{E}_k/\overline{E}_k$	Lower/upper bound on energy level of PEV k (kWh).
E_k^{base}	Minimum energy required to perform round trip of PEV k (kWh).
$I_{k,t}^s$	Arrival and departure indicator of PEV k.
$T_j^{\min}$	Lowest tolerable water temperature in EWH j ($°C$).
T_j^d	Desired water temperature in EWH j ($°C$).
δ_j	Temperature deviation between T_j^d and $T_j^{\min}$ ($°C$).
$\underline{l}_j/\overline{l}_j$	Rated power usage of EWH j (kW).
η_n^+/η_n^-	Efficiency of charging/discharging ES n.
$\underline{E}_n/\overline{E}_n$	Lower/upper bound on energy level of ES n

	(kWh).
P_n^+/P_n^-	Rated charging/discharging power of ES n (kW).
$T_i^{\max}/T_i^{\min}$	Indoor temperature limitations of CB i $(^\circ C)$.
$T_t^{s,\text{out}}$	Outdoor temperature $(^\circ C)$.
Ψ_t^s	Solar irradiance (kW/m^2).
$\sigma_{i,t}$	Cooling/heating indicator of CB i.
α_i, β_i	Temperature coefficients of CB i.
T_i^d	Desired indoor temperature of CB i $(^\circ C)$.
η_i	HVAC system performance coefficient of CB i.
δ_i	Indoor temperature deviation of CB i $(^\circ C)$.

Variables

$T_{i,t}^{s,\text{in}}$	Indoor temperature of CB i $(^\circ C)$.
$T_{i,t}^{s,\text{iw}}$	Inner envelop temperature of CB i $(^\circ C)$.
$T_{i,t}^{s,\text{ow}}$	Outer envelop temperature of CB i $(^\circ C)$.
$P_{i,t}^{s,o}$	Actual power utilized by the HVAC system in CB i (kW).
$P_{i,t}^s$	Power consumed by the HVAC system in CB i (kW).
$C_{i,t}^s$	Comfort level related with the indoor temperature in CB i.
$E_{k,t}^s$	Energy level of PEV k (kWh).
$p_{k,t}^{s,+}$	Charging rate of PEV k (kW).
$u_{k,t}^{s,+}$	Charging indicator of PEV k.
$C_{k,t}^s$	Comfort level related with energy level of PEV k.
$E_{n,t}^s$	ES n's energy level (kWh).
$p_{n,t}^{s,+}/p_{n,t}^{s,-}$	ES n's charging/discharging power (kW).
$u_{n,t}^{s,+}/u_{n,t}^{s,-}$	ES n's charging/discharging indicator.
$h_{j,t}^s$	Heating output of the heat boiler j $(kBtu)$.
$g_{\text{RT},t}^{s,+}/g_{\text{RT},t}^{s,-}$	Power exchange with the real-time retail electricity market (kW).
$g_{\text{DA},t}^-/g_{\text{DA},t}^+$	Power exchange with the day-ahead retail electricity market (kW).
$I_{c,t}$	CHP c's on/off indicator.
$y_{c,t}/z_{c,t}$	CHP c's start-up/shut-down indicator.
$p_{c,t}^s$	Power output of CHP c (kW).
$\delta_t^s, \varepsilon^s, \zeta, \psi_t$	Auxiliary variables.
$l_{j,t}^s$	Power consumption of EWH j (kW).
$T_{j,\tau}^s$	Water temperature of the thermal storage (TS) j $(^\circ C)$.
$C_{j,\tau}^s$	Comfort level related with TS j.

I. Introduction

BUILDINGS consume nearly 40% of the annual electricity generation of the United States (U.S.), of which half of total energy consumption is from commercial buildings (CBs) [1]. CBs contribute to a significant portion of the gross domestic product (GDP) in the U.S. Ensuring the reliability of the CBs is a major concern of distribution system operators (DSOs). However, congestion of transformers and distribution lines in the upstream grid can lead to contingency issues, which pose a significant threat to the reliability of CBs in commercial campuses. To prevent a contingency issue from influencing the reliability of a commercial campus, a controller is needed for the optimal energy management.

Among prior proposed energy management strategies, their objectives can be categorized into three groups: (i) to minimize the operating cost of the system [2]; (ii) to maximize the comfort levels of occupants or minimize the discomfort levels of occupants (mainly related with the indoor temperature) [3]; and (iii) to minimize the load curtailment of the system or maximize the survivability of critical loads [4]. Reference [5] synthetically combines the first two objectives using a stochastic optimization approach. The energy management strategy proposed in [6] considers both operation cost minimization and customer comfort level maximization in a commercial campus. However, the islanding capability of a commercial campus, which is one of the unique features of a microgrid, is not addressed. With the increasing market trend of plug-in electric vehicles (PEVs), an effective energy management system should also handle the uncertainties associated with PEVs [7]. Even though the penetration level of PEV owners among all occupants of CBs is relatively small, the instant charging of PEVs upon arrival can create huge demand ripples, which not only increase the expected operation and maintenance (O&M) costs, but also the possibility of a cascading failure occurring at the point of common coupling (PCC) [8].

The islanding capability of a commercial campus can ensure sufficient energy supply to the critical loads during the uncertain islanding period. Specifically, in the case of microgrid scheduling, the problem of islanding constraints has received considerable attention [9]. A review of existing methods in handling islanding conditions for microgrid central controllers is provided in [10], where the concept of smooth transition between grid-connected mode and islanded mode is discussed. In [11], G. Liu *et al*.present an optimal scheduling model for microgrid operation taking into account the probabilistic constraints of successful islanding. A chance constraint is proposed to represent the probability of a microgrid maintaining enough spinning reserve to accommodate the demand and renewable energy after islanding from the upstream grid. Similarly, a risk-averse method is introduced in [12] for microgrid reconfiguration and reorganization after islanding. The authors in [13], [14] utilize the combined heat and power (CHP) units as back-up power and heating sources along with other major components in a microgrid to overcome the energy imbalance caused by the islanding issues. In addition, the possibilities of losing major components are also considered. Voltage imbalance in the microgrid caused by the islanding from the main grid is studied in [15], which utilizes distributed generators and inverters to maintain the voltage magnitude in the islanded mode. Z. Li *et al*.demonstrate an islanding-aware economic dispatch mechanism for the microgrid central controller to minimize the operating cost in both grid-connected mode and islanded mode [16]. They also present the concept of energy deviation along with its associated costs. None of the aforementioned works, however, has considered all the distinct factors for the optimal energy management strategy of a commercial campus with islanding capabilities.

In this paper, we propose an optimal risk-constrained energy

management strategy for campus-based CBs with islanding capabilities taking into consideration comprehensive comfort levels of the occupants. The objective is to minimize expected O&M costs, while maximizing comprehensive comfort levels for CB occupants. A two-stage risk-constrained scenario-based stochastic optimization approach is developed to handle various uncertainties associated with the energy management process, such as power generation of roof-top solar panels, arrival state-of-charges (SoCs) and arrival/departure time of PEVs, intermittent load demand in the CBs, and uncertain grid-connection conditions. These uncertainties can lead to the final decision of providing both the lowest expected operating costs and the highest standard deviation in the solution distribution. In order to handle such risk, a conditional-value-at-risk (CVaR) method is adopted to provide the risk-averse energy management strategy based on the selected risk-aversion parameters and confidence levels. A scenario reduction method is leveraged to reduce the computational burden while maintaining accuracy of the stochastic programming. Extensive simulation results validate the effectiveness of the proposed energy management strategy in minimizing the total O&M costs of CBs with islanding capabilities, while maximizing the comprehensive comfort levels of the occupants.

The main contributions of this paper are as follows.

1) An optimal risk-constrained energy management strategy for campus-based CBs considering the occupants' comfort level as well as islanding uncertainty is proposed.
2) A CVaR method is introduced to manage the risks and handle all the uncertainties.
3) Extensive simulation results based on real-world data sets are presented to validate the effectiveness of the proposed energy management strategy.

The rest of the paper is organized as follows. In Section II, a high level structure of the commercial campus is introduced, where the detailed constraints of major components are formulated. Section III presents the mathematical formulation of the proposed two-stage risk-constrained scenario-based stochastic optimization problem and the solution algorithm to reformulate the multi-objective problem into a mixed-integer linear program (MILP). We perform several case studies in Section IV and then draw conclusions in Section V.

II. System Modeling

In this section, we first describe the overall scheme of the commercial campus that we considered in this paper. Then, we introduce the detailed formulations of the major components shown in Fig. 1.

A. Commercial Campus

The commercial campus consists of several CBs, CHP units, and parking lots with PEV chargers as shown in Fig. 1. Each CB has the following major components: (i) one HVAC system; (ii) one electric water heater and one gas-based heater that share the same hot water tank, i.e., a thermal storage (TS); (iii) ES units; and (iv) base loads (critical loads that cannot be curtailed), including

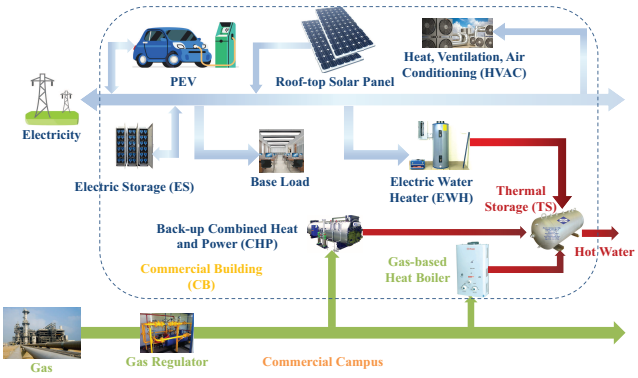

Fig. 1. Example of a commercial campus.

lights, servers, desktops, refrigerators, fans, etc. Some of the CBs' occupants own PEVs that require charging during regular office hours.

1) Electrical Storage: One of major components considered in a system to mitigate power imbalances caused by uncertainties is the electrical storage (ES) unit [17]. In addition to maintaining the power balance, the ES unit also provides up/down islanding capability based on reserve, which will be introduced in Section II-C. First, the energy dynamics of the ES unit n is formulated as follows:

$$E^s_{n,t} = E^s_{n,t-1} + p^{s,+}_{n,t}\eta^+_n t - \frac{p^{s,-}_{n,t} t}{\eta^-_n}, \forall n, t, s, \tag{1}$$

where the energy level $E^s_{n,t}$ depends on the energy level of the previous time step $E^s_{n,t-1}$ and the energy charging/discharging into/from the ES unit k during the current time step.

Second, the lower and upper bounds on the ES unit n's energy level are modeled in the following:

$$\underline{E}_n \le E^s_{n,t} \le \overline{E}_n, \;\; E^s_{n,1} = E^s_{n,T}, \forall n, t, s. \tag{2}$$

Specifically, the final energy level in the operating day is set to be the same as the initial energy level [18].

Third, the charging and discharging decisions of ES unit n are modeled based on binary variables $u^{s,+}_{n,t}$ and $u^{s,-}_{n,t}$ as follows:

$$\begin{aligned} &0 \le p^{s,+}_{n,t} \le P^+_n u^{s,+}_{n,t}, \;\; 0 \le p^{s,-}_{n,t} \le P^-_n u^{s,-}_{n,t}, \forall n, t, s \\ &0 \le u^{s,+}_{n,t} + u^{s,-}_{n,t} \le 1, \forall n, t, s, \end{aligned} \tag{3}$$

where charging and discharging processes cannot occur in the same time slot.

2) PEVs: The instant charging demand of PEVs requires that charging the vehicles be spread over set time intervals and in relation to real-time electricity prices. Energy management methods such as demand response (DR) are being leveraged to avoid the aforementioned charging ripples, where charging demand of PEVs are treated as both shiftable and interruptable [19]. Even though the arrival SoCs and the arrival/departure time of the PEVs are uncertain, the PEVs should be charged to the desired SoCs as required by the occupant in not only grid-connected mode but also

islanded mode. Therefore, we formulate the energy dynamics of PEVs as follows:

$$E^s_{k,t} = E^s_{k,t-1} + p^{s,+}_{k,t}\eta^+_k t, \forall k, t, s, \tag{4}$$

where the energy gap between two consecutive time slots is based on the charging rate $p^{s,+}_{k,t}\eta^+_k t$ of the PEV k.

In addition, the physical limitations on the energy level of the PEV k is modeled as follows:

$$\underline{E}_k \leq E^s_{k,t} \leq \overline{E}_k, \forall k, t, s. \tag{5}$$

With the purpose of providing reliable power to the PEVs in both grid-connected and islanded mode, the charging process of the PEV k is modeled in the following constraint:

$$0 \leq p^{s,+}_{k,t} \leq P^+_k I^s_{k,t} u^{s,+}_{k,t}, \forall k, t, s, \tag{6}$$

where parameter $I^s_{k,t}$ denotes the uncertain arrival and departure status of the PEV k as binary parameters $\{0, 1\}$. Parameter $I^s_{k,t} = 1$ when the PEV k is at the charger in the parking lot; parameter $I^s_{k,t} = 0$ when the PEV k is absent. Binary variable $u^{s,+}_{k,t}$ is proposed to capture the charging decision of the PEV k.

3) Combined Heat and Power Units: In order to provide sufficient electricity to the commercial campus in both the islanded mode and the grid-connected mode, gas-based combined heat and power (CHP) units are deployed [20]. The CHPs stay idle before the business day to meet the operation restrictions. Due to the physical limitations, the actual power generation from CHP c is regulated by both the minimum on power and the rated power:

$$\underline{P}_c I_{c,t} \leq p^s_{c,t} \leq \overline{P}_c I_{c,t}, \forall c, t, s. \tag{7}$$

Specifically, the power generation of CHP c is zero when the CHP c is off, i.e., $I_{c,t} = 0$.

In addition, based on the on/off status of CHP c and the start-up/shut-down indicator, the ramping limitations can be expressed as follows:

$$\begin{aligned} p^s_{c,t} - p^s_{c,t-1} &\leq \mathrm{RU}_c I_{c,t-1} + \overline{P}_c(1 - I_{c,t}) + \overline{P}_{SU} y_{c,t}, \forall c, t, s \\ p^s_{c,t-1} - p^s_{c,t} &\leq \mathrm{RD}_c I_{c,t} + \overline{P}_c(1 - I_{c,t-1}) + \overline{P}_{SD} z_{c,t}, \forall c, t, s. \end{aligned} \tag{8}$$

Moreover, the CHP needs to be cooled down for a certain period of time before it is ready to be turned on again, and vice versa. Therefore, we have following minimum up/down time constraints:

$$\sum_{\tau=t}^{t+\mathrm{UT}_c-1} I_{c,\tau} \geq \mathrm{UT}_c y_{c,t}, \quad \sum_{\tau=t}^{t+\mathrm{DT}_c-1} (1 - I_{c,\tau}) \geq \mathrm{DT}_c z_{c,t}, \forall c, t. \tag{9}$$

The CHP cannot start-up and shut-down at the same time, which is modeled by the following unit commitment constraints:

$$I_{c,t} - I_{c,t-1} = y_{c,t} - z_{c,t}, \ y_{c,t} + z_{c,t} \leq 1, \forall c, t. \tag{10}$$

4) HVAC System: HVAC systems are installed in CBs to provide either cooling or heating for the occupants. A third order state-space equation is leveraged to model the relationship of the indoor temperature, the inner wall temperature, the outer wall temperature, the solar irradiance, the outdoor temperature, and the power consumption of the HVAC system [21]:

$$T^s_{i,t+1} = \beta_i T^s_{i,t} + \alpha_i V^s_{i,t}, T^{s,\text{in}}_{i,t} = \Gamma T^s_{i,t}, \forall i, t, s, \tag{11}$$

where $T^s_{i,t} = [T^{s,\text{in}}_{i,t}, T^{s,\text{iw}}_{i,t}, T^{s,\text{ow}}_{i,t}]^T$ is a state vector that contains the indoor temperature, the inner wall temperature, and the outer wall temperature. $V^s_{i,t} = [T^{s,\text{out}}_t, \Psi^s_t, \sigma_{i,t} P^{s,o}_{i,t}]^T$ is a state/decision vector that indicates the influences from the outdoor temperature, the solar irradiance, and the power consumption of the HVAC system, respectively. Variable $P^{s,o}_{i,t} = \eta_i P^s_{i,t}$ is the actual power utilized by the HVAC system. α_i and β_i are parameters based on the physical structure of the CB i, such as the fraction of solar irradiation entering inner walls, the effective window area, the thermal resistance data, and the thermal capacitance. Parameter $\sigma_{i,t}$ determines the heating/cooling mode of the HVAC system, where $\sigma_{i,t} = 1$ in winter and $\sigma_{i,t} = -1$ in summer. We set $\Gamma = [1, 0, 0]$ to focus on the indoor temperature.

In addition, with the help of HVAC system, the desired indoor temperature can be achieved by equation (12).

$$T^d_i - \delta_i \leq T^{s,\text{in}}_{i,t} \leq T^d_i + \delta_i, \forall i, t, s, \tag{12}$$

where the desired indoor temperature is denoted by T^d_i. Parameter δ_i represents the tolerable temperature deviation of commercial building i. Even though the occupants of the CB want to have the desired indoor temperature as soon as possible, however, the capability of the HVAC in adjusting the indoor temperature is restricted by its power consumption as shown in constraint (13).

$$0 \leq P^s_{i,t} \leq \overline{P}_i, \forall i, t, s, \tag{13}$$

where $\overline{P}_i$ represents the upper bound of the i-th HVAC system's power consumption.

5) Heat Boiler: In case the hot water demand cannot be met by the CHPs and EWHs, the heat boiler is installed in the commercial campus to supply sufficient hot water to the CBs, especially when the gas station is still working properly and the commercial building is disconnected from the main grid:

$$0 \leq h^s_{j,t} \leq \overline{H}_j, \forall j, t, s, \tag{14}$$

where hot water supplied by the heat boiler $h^s_{j,t}$ is restricted by its physical limitation $\overline{H}_j$.

6) Electric Water Heater and Thermal Storage Unit: The total energy L^s_j consumed by the EWH j in the operating day is predefined by the central controller based on the historical data, where the power consumption of EWH j is treated as deferrable within a certain time interval $[t^a_j, t^d_j]$. Moreover, the power consumption of the EWH j is restricted to be zero outside of the time interval

$[t_j^a, t_j^d]$. Thus, we can model the unique features of the EWHs as follows:

$$\sum_{t=t_j^a}^{t_j^d} l_{j,t}^s = L_j^s, \underline{l}_j \le l_{j,t}^s \le \overline{l}_j, \forall j, t \in [t_j^a, t_j^d], s$$
$$l_{j,t}^s = 0, \forall j, t \notin [t_j^a, t_j^d], s. \quad (15)$$

The exhausted heat of the CHP units is utilized to satisfy part of the hot water demand through heating the hot water tank with a power-to-heat ratio ζ_c. Moreover, the water temperature of the hot water tank $T_{j,\tau}^s$ is determined by both the initial water temperature $T_{j,0}^s$ and the temperature deviation between different time slots ΔT_j^s. Specifically, the water temperature deviation contains the incremental temperature deviation from the hot water of EWHs, CHP units and heat boilers, and the decremental temperature deviation from the losses into ambient temperature $H_{j,t}^{\text{de}}$. Thus, the detailed water temperature dynamics in the TS unit j is modeled as follows:

$$T_{j,\tau}^s = T_{j,0}^s + \Delta T_j^s, \forall j, \tau, s \quad (16)$$
$$\Delta T_j^s = \sum_{t=1}^{\tau} \frac{\zeta_j l_{j,t}^s + h_{j,t}^s + \zeta_c p_{c,t}^s - H_{j,t}^{\text{de}}}{M_j C_{\text{water}}}, \forall j, \tau, s.$$

B. Retail Electricity Market

A two-settlement pool-based retail electricity market is considered. Prior to the operating day, the commercial campus central controller bids in the day-ahead electricity market with all the uncertainties unknown. Then the system operator clears the electricity market at $10pm$ with the day-ahead buying and selling prices. In the operating day, the system operator clears the electricity market at the beginning of each time slot, with the real-time electricity price. All uncertainties are unveiled at the beginning of the operating day. A penalty occurs when the day-ahead bidding amount and the real-time exchange amount are different. In addition, the power exchange through the PCC is regulated by the physical limitations. The power exchange limitation on the PCC can be modeled as follows:

$$0 \le g_{\text{DA},t}^- \le \overline{g},\ 0 \le g_{\text{DA},t}^+ \le \overline{g}, \forall t$$
$$0 \le g_{\text{RT},t}^{s,-} \le \overline{g},\ 0 \le g_{\text{RT},t}^{s,+} \le \overline{g}, \forall t, s. \quad (17)$$

C. Islanding Capability Based Reserve

In order to provide optimal day-ahead decisions, all dispatchable DERs in the commercial campus are utilized to satisfy the minimum reserve requirement to maintain the islanding capability of the campus [22]. In the proposed model, the one time slot backup is guaranteed. During that time, the minimum requirement for the power spinning reserve is to compensate the real-time power exchange between the main grid and the commercial campus. Variables $P_{re,t}^{s,+}$ and $P_{re,t}^{s,-}$ are introduced as islanding capability based reserves, as follows: (i) power scheduled to buy from the retail electricity market during day-ahead but cannot deliver in the real-time; and (ii) power scheduled to sell to the retail electricity market in the day-ahead but cannot deliver in the real-time. Since only controllable and dispatchable components are considered for the islanding capability based reserve [23], charging of ES units, ramping-down of CHP units, and deferrable loads can contribute to the selling reserve $P_{re,t}^{s,-}$; discharging of ES units and ramping-up of CHP units can contribute to the selling reserve $P_{re,t}^{s,+}$. We further denote the reserve variables for the aforementioned components as follows: variable $p_{c,t}^{RU,s}/p_{c,t}^{RD,s}$ as the ramping-up/ramping down reserve of CHP unit c; variable $p_{n,t}^{re,s,+}$ as the reserve from charging of ES unit n; variable $p_{n,t}^{re,s,-}$ as the reserve from discharging of ES unit n; and $l_{j,t}^{re,s}$ as the reserve from the EWH j, respectively.

The constraints related to the islanding capability based reserve can be expressed in the following formulations:

$$P_{re,t}^{s,+} = \sum_{i=1}^{N_i}\sum_{c=1}^{N_i^c} p_{c,t}^{RU,s} + \sum_{i=1}^{N_i}\sum_{n=1}^{N_i^n} p_{n,t}^{re,s,-}, \forall t, s$$
$$P_{re,t}^{s,-} = \sum_{i=1}^{N_i}\sum_{c=1}^{N_i^c} p_{c,t}^{RD,s} + \sum_{i=1}^{N_i}\sum_{n=1}^{N_i^n} p_{n,t}^{re,s,+} + \sum_{i=1}^{N_i}\sum_{j=1}^{N_i^j} l_{j,t}^{re,s},$$
$$\forall t \in [t_j^a, t_j^d], s$$
$$P_{re,t}^{s,-} = \sum_{i=1}^{N_i}\sum_{c=1}^{N_i^c} p_{c,t}^{RD,s} + \sum_{i=1}^{N_i}\sum_{n=1}^{N_i^n} p_{n,t}^{re,s,+}, \forall t \notin [t_j^a, t_j^d], s. \quad (18)$$

In addition, the relationship between the islanding capability based reserve and the day-ahead power exchange schedule can be formulated as follows:

$$P_{re,t}^{s,+} \ge g_{\text{DA},t}^+,\ P_{re,t}^{s,-} \ge g_{\text{DA},t}^-, \forall t, s. \quad (19)$$

Furthermore, for each aforementioned component, the islanding capability based reserves have following upper/lower bounds:

$$p_{c,t}^{RU,s} \le \text{RU}_c I_{c,t-1} + \overline{P}_c(1 - I_{c,t}) + \overline{P}_{SU} y_{c,t}, \forall c, t, s$$
$$p_{c,t}^{RU,s} \le \overline{P}_c I_{c,t} - p_{c,t}^s, \forall c, t, s$$
$$p_{c,t}^{RD,s} \le \text{RD}_c I_{c,t} + \overline{P}_c(1 - I_{c,t-1}) + \overline{P}_{SD} z_{c,t}, \forall c, t, s$$
$$p_{c,t}^{RD,s} \le p_{c,t}^s - \underline{P}_c I_{c,t}, \forall c, t, s$$
$$p_{n,t}^{re,s,-} \le P_n^- u_{n,t}^{s,-},\ \frac{p_{n,t}^{re,s,-}}{\eta_n^-} \le E_{n,t}^s - \underline{E}_n, \forall n, t, s \quad (20)$$
$$p_{n,t}^{re,s,+} \le P_n^+ u_{n,t}^{s,+},\ p_{n,t}^{re,s,+}\eta_n^+ \le \overline{E}_n - E_{n,t}^s, \forall n, t, s$$
$$l_{j,t}^{re,s} \le \overline{l}_j,\ l_{j,t}^{re,s} \le L_j^s - \sum_{t_j^a}^{t} l_{j,t}^s, \forall t \in [t_j^a, t_j^d], s.$$

D. Energy Balance

The energy balance considered in this paper is two fold: power balance and hot water balance. Due to the limited capacity and the proximity of load and generation in a commercial campus, the network is typically not the limiting constraint. Therefore, we neglected the network constraints and leveraged the one node model to ensure sufficient power and hot water supply to the end users in the commercial campus.

1) Power Balance: As shown in Fig. 1, the major components in each CB can be classified into three types: (i) purely power consumer, i.e., HVAC systems; (ii) purely power provider, i.e., renewables; and (iii) semi-consumer/semi-provider (also known as prosumer), i.e., ES units. In order to maintain the power balance, the power supply must be equal to the power demand. Thus, on the left hand side of equation (21), we have the power output of ES units, power output of renewables, power buying from the main grid in real-time, and power output of CHP units; on the right hand side of equation (21), we have power selling to the main grid in real-time, power consumption of aggregated base load, power consumption of EWHs, power consumption of HVAC systems, and power consumption of PEVs.

$$\begin{aligned}&\sum_{i=1}^{N_i}\sum_{n=1}^{N_i^n}\left(p_{n,t}^{s,-}-p_{n,t}^{s,+}\right)+\sum_{i=1}^{N_i}\sum_{m=1}^{N_i^m}w_{m,t}^{s}+g_{\text{RT},t}^{s,+}+\sum_{i=1}^{N_i}\sum_{c=1}^{N_i^c}p_{c,t}^{s}\\ =&g_{\text{RT},t}^{s,-}+D_t^s+\sum_{i=1}^{N_i}\sum_{j=1}^{N_i^j}l_{j,t}^{s}+\sum_{i=1}^{N_i}P_{i,t}^{s}+\sum_{i=1}^{N_i}\sum_{k=1}^{N_i^k}p_{k,t}^{s,+},\forall t,s.\end{aligned}\tag{21}$$

2) Hot Water Balance: In our model, hot water can be stored in the TS unit and dispatched to the occupants through the pipes without heat loss. The hot water is supplied by three major components: CHP units, EWHs, and hot boilers. Similarly, we have the hot water balance constraints as follows:

$$\zeta_c\sum_{i=1}^{N_i}\sum_{c=1}^{N_i^c}p_{c,t}^{s}+\zeta_j\sum_{i=1}^{N_i}\sum_{j=1}^{N_i^j}l_{j,t}^{s}+\sum_{i=1}^{N_i}\sum_{j=1}^{N_i^j}h_{j,t}^{s}\geq Q_t^s,\forall t,s.\tag{22}$$

Unlike the power constraint where the power supply must equal to the power demand, we assume that the surplus hot water can be discarded without penalty.

E. Conditional Value at Risk

In the proposed scenario-based two-stage stochastic optimization approach, the O&M costs of each scenario is a random variable that involves the aforementioned uncertainties. In the scenario-based O&M costs distribution, there are optimal strategies with huge O&M costs for the worst-case scenarios that have rather small possibilities to occur. Therefore, a risk aversion approach is needed to avoid such issue, which can ensure that the cost variability is minimized as desired [24]. In our model, the variability among all scenario-based O&M costs is handled by a CVaR method. In the CVaR, the risk of the proposed problem is minimized though minimizing the scenarios with O&M costs larger the $(1-\epsilon)$–quantile of the O&M costs distribution, i.e., value-at-risk (VaR) ζ, where ϵ is the confidence level [25]. The relationship between the VaR and the O&M costs can be represent through the following constraints:

$$\varepsilon^s\geq \text{oc}^s-\zeta,\ \varepsilon^s\geq 0,\forall s.\tag{23}$$

In the proposed model, we use oc^s to represent the O&M costs of scenario s. Non-negative auxiliary variable ε^s denotes the deviation between the O&M costs and the VaR.

F. Comfort Levels

To model the consumers' comfort level with respect to an HVAC system, we leverage piecewise linearization.

$$C_{i,t}^{s}=\begin{cases}0, & T_{i,t}^{s,\text{in}}\geq T_i^{\max},\\ \frac{T_i^{\max}-T_{i,t}^{s,\text{in}}}{\delta_i-\epsilon_i}, & T_i^d+\epsilon_i\leq T_{i,t}^{s,\text{in}}\leq T_i^{\max},\\ 1, & T_i^d-\epsilon_i\leq T_{i,t}^{s,\text{in}}\leq T_i^d+\epsilon_i,\\ \frac{T_{i,t}^{s,\text{in}}-T_i^{\min}}{\delta_i-\epsilon_i}, & T_i^{\min}\leq T_{i,t}^{s,\text{in}}\leq T_i^d-\epsilon_i,\\ 0, & T_{i,t}^{s,\text{in}}\leq T_i^{\min}.\end{cases}\tag{24}$$

As provided in (24), the comfort level related to the HVAC system is measured with the actual indoor temperature $T_{i,t}^{s,\text{in}}$ and the desired indoor temperature T_i^d. As the indoor temperature varies within its upper bound $T_i^{\max}$ and lower bound $T_i^{\min}$, the comfort level varies in the range of $[0,1]$. Comfort level equals to 1, representing the most comfort situation, i.e., the indoor temperature is maintained within the desired range, and it equals to 0, indicating the most discomfort, i.e., the indoor temperature has reached the upper or lower bound. Since the human body cannot sense small temperature deviation denoted by ϵ_i, the range between $T_i^d+\epsilon_i$ and $T_i^d-\epsilon_i$ is treated as the most comfortable region.

Moreover, the comfort level related to the PEVs is modeled based on the energy level of the PEVs.

$$C_{k,t}^{s}=\begin{cases}1, & E_k^d\leq E_{k,t}^s,\\ \frac{E_{k,t}^s-E_k^{\text{base}}}{E_k^d-E_k^{\text{base}}}, & E_k^{\text{base}}\leq E_{k,t}^s\leq E_k^d,\\ 0, & E_{k,t}^s\leq E_k^{\text{base}}.\end{cases}\tag{25}$$

The E_k^{base} is a basic requirement, which is the energy for a round trip between the house and the commercial campus. Similarly, the comfort level is restricted in the range of $[0,1]$, where 1 represents the most comfort status, i.e., the PEV is fully charged ($95\%SoC$) and 0 denotes the most discomfort status, i.e., the PEV k reaches the base energy level, respectively.

In addition, the comfort level related to water temperature is modeled as follows:

$$T_j^d-\delta_j\leq T_{j,\tau}^s\leq T_j^d+\delta_j,\forall j,\tau,s\tag{26}$$

$$C_{j,\tau}^{s}=\begin{cases}1, & T_j^d\leq T_{j,\tau}^s,\\ \frac{T_{j,\tau}^s-T_j^{\min}}{T_j^d-T_j^{\min}}, & T_j^{\min}\leq T_{j,\tau}^s\leq T_j^d,\\ 0, & T_{j,\tau}^s\leq T_j^{\min}.\end{cases}\tag{27}$$

Similarly, the comfort level is restricted within the range of $[0,1]$, where 1 represents the most comfort status and 0 denotes the most discomfort status, respectively.

III. Problem Formulation and Solution Algorithm

A. Problem Formulation

In this section, we formulate the optimal energy management problem into a two-stage risk-constrained stochastic programming. The multi-objective function is formulated from two aspects: (i)

minimizing the expected O&M costs of the commercial campus with islanding capabilities; and (ii) maximizing the comfort levels of the occupants in the CBs. However, these proposed functions aim at conflicting objectives, where the minimization and maximization cannot be added together without transformation. In addition, the scale of the two formulations is different; therefore, a unification of both objective functions is implemented. Instead of simply adding weighting factors, we determine the scale-down parameter P_{base} based on the power that is consumed to increase the total comfort levels from minimum to maximum, i.e., from 0 to 1. After unification, we change the minimization of the expected O&M costs into maximizing the expected revenue of the commercial campus.

1) Objective Function Related to O&M costs: The first part of the proposed risk-constrained two-stage stochastic formulation aims to minimize the expected O&M costs of a commercial campus:

$$\begin{aligned}
\min & \sum_{t=1}^{N_t}\sum_{c=1}^{N_c}\left(\mathrm{SU}_c y_{c,t}+\mathrm{SD}_c z_{c,t}\right)\\
&+\sum_{s=1}^{N_s}\rho_s\sum_{t=1}^{N_t}\Bigg\{\sum_{c=1}^{N_c}(\beta_c p^s_{c,t}+\gamma_c I_{c,t})\\
&+c^{s,+}_{\mathrm{DA},t}g^{+}_{\mathrm{DA},t}-c^{s,-}_{\mathrm{DA},t}g^{-}_{\mathrm{DA},t}\\
&+c^{s}_{\mathrm{RT},t}\left[g^{s,+}_{\mathrm{RT},t}-g^{+}_{\mathrm{DA},t}-\left(g^{s,-}_{\mathrm{RT},t}-g^{-}_{\mathrm{DA},t}\right)\right]\\
&+c^{p}_{t}\left(\left|g^{+}_{\mathrm{DA},t}-g^{s,+}_{\mathrm{RT},t}\right|+\left|g^{-}_{\mathrm{DA},t}-g^{s,-}_{\mathrm{RT},t}\right|\right)\\
&+\sum_{i=1}^{N_i}\sum_{n=1}^{N^n_i}c_n\left(p^{s,+}_{n,t}\eta^{+}_{n}+\frac{p^{s,-}_{n,t}}{\eta^{-}_{n}}\right)\\
&+\sum_{i=1}^{N_i}\sum_{j=1}^{N^j_i}c^{b}_{t}h^{s}_{j,t}\Bigg\}\\
&+\kappa\left(\zeta+\frac{1}{1-\epsilon}\sum_{s=1}^{N_s}\rho^s\varepsilon^s\right)
\end{aligned}\tag{28}$$

subject to constraints (1)–(23). The first line of equation 28 models the start-up and shut-down costs of CHP units, where SU_c is the start-up cost, SD_c is the shut-down cost. The second line captures the generation cost of the CHP units, where γ_c is the minimum up cost, β_c is the diesel cost. The third line represents the day-ahead electricity exchange cost, where $c^{s,+}_{\mathrm{DA},t}$ is the day-ahead buying price, $c^{s,-}_{\mathrm{DA},t}$ is the day-ahead selling price. The fourth line expresses the real-time electricity exchange cost, where $c^{s}_{\mathrm{RT},t}$ is the real-time electricity price. The fifth line denotes the penalty for the difference between the day-ahead schedule and the real-time actual power exchange, where c^{p}_{t} is the penalty cost. The sixth line is the degradation cost of the ES units when charging and discharging, where c_n is the degradation cost. The seventh line is the generation cost of heat boilers, where c^{b}_{t} is the gas price. The last line is the risk management cost, where κ is a risk-averse parameter that represents the conservativeness of the central controller.

2) Objective Function Related to Comfort Levels: The second part of the proposed risk-constrained two-stage stochastic formulation aims to maximize the expected comfort levels of the occupant in the CBs:

$$\max\sum_{s=1}^{N_s}\rho_s\sum_{i=1}^{N_i}\left[\sum_{t=1}^{N_t}\left(C^{s}_{i,t}+\sum_{j=1}^{N^j_i}C^{s}_{j,t}\right)+\sum_{t=72}^{80}\frac{N_k}{N_p}\sum_{k=1}^{N_k}C^{s}_{k,t}\right]\tag{29}$$

subject to constraints (24)–(27). The comfort levels include the ones related to the HVAC systems (indoor temperature), to PEVs (SoCs), and to hot water tanks (water temperature). The comfort level related to PEVs is regulated by a penetration level between the total population and the PEV owners in the commercial campus. In addition, unlike the comfort levels related to indoor temperature and water temperature, the occupants care about the SoCs of their PEVs when they are leaving the commercial campus. However, the departure time of the occupants is uncertain, which is assumed to follow a normal distribution between 6:00 pm–8:00 pm. Therefore, we set a proper range (from 6:00 pm to 8:00 pm, i.e., 72 time steps to 80 time steps) for the PEVs' departure starting and ending time slots based on the assumption.

3) Problem Reformulation: The multi-objective problem can be reformulated using the aforementioned methods and formulated into a two-stage scenario-based stochastic programming:

$$\begin{aligned}
\max & -\sum_{t=1}^{N_t}\sum_{c=1}^{N_c}\left(\mathrm{SU}_c y_{c,t}+\mathrm{SD}_c z_{c,t}\right)\\
&+\sum_{s=1}^{N_s}\rho_s\sum_{t=1}^{N_t}\Bigg\{-\sum_{c=1}^{N_c}(\frac{\beta_c p^s_{c,t}}{P_{base}}+\gamma_c I_{c,t})\\
&+\frac{c^{s,-}_{\mathrm{DA},t}g^{-}_{\mathrm{DA},t}}{P_{base}}-\frac{c^{s,+}_{\mathrm{DA},t}g^{+}_{\mathrm{DA},t}}{P_{base}}\\
&+\frac{c^{s}_{\mathrm{RT},t}\left(g^{s,-}_{\mathrm{RT},t}-g^{-}_{\mathrm{DA},t}-g^{s,+}_{\mathrm{RT},t}+g^{+}_{\mathrm{DA},t}\right)}{P_{base}}-\frac{c^{p}_{t}\psi^{s}_{t}}{P_{base}}\\
&-\sum_{i=1}^{N_i}\sum_{j=1}^{N^j_i}c^{b}_{t}h^{s}_{j,t}/\overline{H}_j-\sum_{i=1}^{N_i}\sum_{n=1}^{N^n_i}\frac{c_n\left(p^{s,+}_{n,t}\eta^{+}_{n}+\frac{p^{s,-}_{n,t}}{\eta^{-}_{n}}\right)}{P_{base}}\\
&+\sum_{i=1}^{N_i}C^{s}_{i,t}+\sum_{i=1}^{N_i}\sum_{j=1}^{N^j_i}C^{s}_{j,t}\Bigg\}+\frac{N_k}{N_p}\sum_{s=1}^{N_s}\rho_s\sum_{t=72}^{80}\sum_{k=1}^{N_k}C^{s}_{k,t}\\
&-\kappa\left(\zeta+\frac{1}{1-\epsilon}\sum_{s=1}^{N_s}\rho^s\varepsilon^s\right),
\end{aligned}\tag{30}$$

subject to constraints (1)–(27). ψ_t is an auxiliary variable that replaces the absolute term $\left(\left|g^{+}_{\mathrm{DA},t}-g^{s,+}_{\mathrm{RT},t}\right|+\left|g^{-}_{\mathrm{DA},t}-g^{s,-}_{\mathrm{RT},t}\right|\right)$ in the previous objective function (28), where $\psi^s_t=\psi^s_{1,t}+\psi^s_{2,t}$, $\psi^s_{1,t}=\left|g^{+}_{\mathrm{DA},t}-g^{s,+}_{\mathrm{RT},t}\right|$ and $\psi^s_{2,t}=\left|g^{-}_{\mathrm{DA},t}-g^{s,-}_{\mathrm{RT},t}\right|$.

B. Stochastic Programming

We developed a scenario-based two-stage risk-constrained stochastic programming to handle uncertainties related to the power output of RES units, PEVs' arrival SoCs, PEVs' arrival and

departure time slots, intermittent load demand, grid-connection conditions, and day-ahead and real-time electricity prices. The detailed real-time data of the aforementioned variables cannot be perfectly forecasted prior the operating day. However, with the help of historical data and the stochastic programming, the central controller can obtain the trend of the uncertainties and make optimal decisions. $1,000,000$ scenarios with the same probability are generated containing all the information of the uncertainties, which is impossible for the cental controller of a commercial campus to handle. Therefore, a scenario reduction method is employed to reduce such huge amount of scenarios that can still maintain a certain level of optimality comparing to original data [26].

In addition to scenario reduction process, there is still one more step before the problem can be handled by commercial solvers: linearization. As shown in the objective function, the absolute terms $\psi^s_{1,t} = \left|g^+_{\text{DA},t} - g^{s,+}_{\text{RT},t}\right|$ and $\psi^s_{2,t} = \left|g^-_{\text{DA},t} - g^{s,-}_{\text{RT},t}\right|$ need to be linearized as follows:

$$\psi^s_{1,t} \geq g^+_{\text{DA},t} - g^{s,+}_{\text{RT},t},\ \psi^s_{1,t} \geq g^{s,+}_{\text{RT},t} - g^+_{\text{DA},t}, \forall t, s \tag{31}$$

$$\psi^s_{2,t} \geq g^-_{\text{DA},t} - g^{s,-}_{\text{RT},t},\ \psi^s_{2,t} \geq g^{s,-}_{\text{RT},t} - g^-_{\text{DA},t}, \forall t, s. \tag{32}$$

In this way, the scenario-based two-stage risk-constrained stochastic programming is formulated as a mixed-integer linear programming (MILP), which is able to be solved by commercial solvers such as GUROBI. Specifically, there are $962,952$ rows, $1,115,649$ columns, and $6,833,905$ non-zeros in the optimization model, with $792,225$ continuous variables and $323,424$ integer variables ($323,424$ binary variables).

IV. Simulation Results

We evaluate the proposed algorithm through real-world datasets. The detailed data has been described in the first place and then the performance of the proposed framework has been tested.

A desktop computer with 3.0 GHz Intel Core i5-7400 CPU and 8GB RAM is used as the simulation tool, where Python 2.7 and GUROBI 8.0.0 are major softwares implementing the MILP and the solver. A convergence criterion is set as the MIPGAP default value (0.0001).

A. Numerical Settings

The proposed system is tested in a commercial campus with six CBs, three CHPs, and fifty charging piles for PEVs in total. In each CB, there is one HVAC system, one TS, one EWH, one heat boiler, one ES, one pack of roof-top solar panels, and one base load. All parameters are unified for computational proposes, with P_{base} at $1,867kW$ and H_{base} at $1,224kBtu$. Comfort levels are only considered during the business hours when occupants are in the CBs (from 8 a.m. to 8 p.m.), where the parameters for comfort levels related components are from [6]. The data for the base load and the hot water demand are from [6] as well. The entire operating day contains 24 hours. Each hour is separated into 4 time slots.

The parameters for CHPs are from [27]. The total capacity of the installed solar panels is $360kW$, where the historic generation patterns, solar irradiance and outdoor temperature data are from [28], with proper scaling coefficients. The electricity prices are from [29], with proper scaling coefficients. The upper bound on the tie-line between the commercial campus and the main grid is set as $1,867kW$, which is the same as the base power P_{base}. We set the selling price at 80% of the buying price in the day-ahead electricity market.

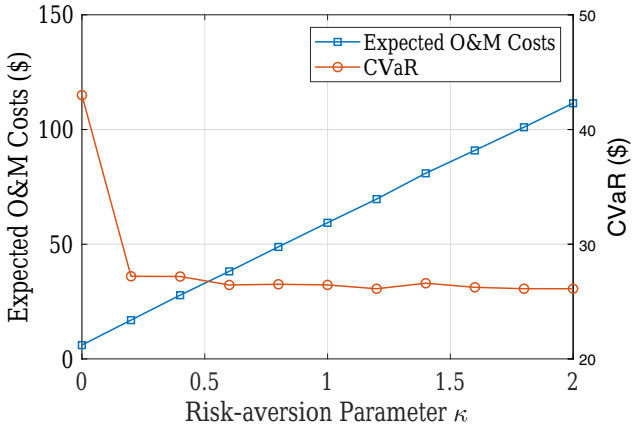

Fig. 2. The expected O&M costs and CVaR of the commercial campus with different risk-aversion parameters for 89% confidence level.

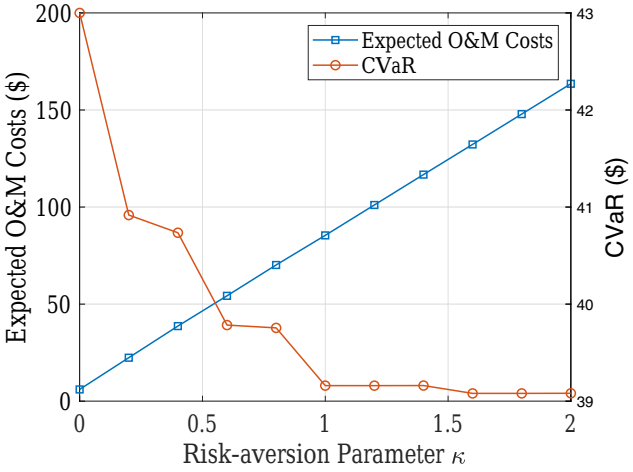

Fig. 3. The expected O&M costs and CVaR of the commercial campus with different risk-aversion parameters for 99% confidence level.

B. Case Study

We evaluate the proposed optimal energy management strategy from mainly three aspects: (i) to show the convergence rate for a large-scale MILP, and the CVaR and expected O&M costs based on various risk-constrained parameters; (ii) to select the proper risk-management parameters based on the simulation results and get the first-stage decisions; and (iii) to test the islanding capability of the commercial campus with and without the reserve constraints under uncertain grid-connection conditions, discuss the influence on second-stage decisions and the O&M costs.

1) Convergence Rate, CVaR and Expected Operation and Maintenance Costs: The proposed optimal energy management strategy

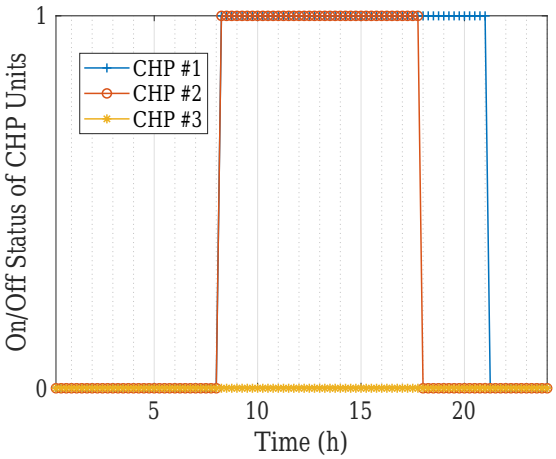

Fig. 4. The day-ahead On/Off decisions for the CHP units.

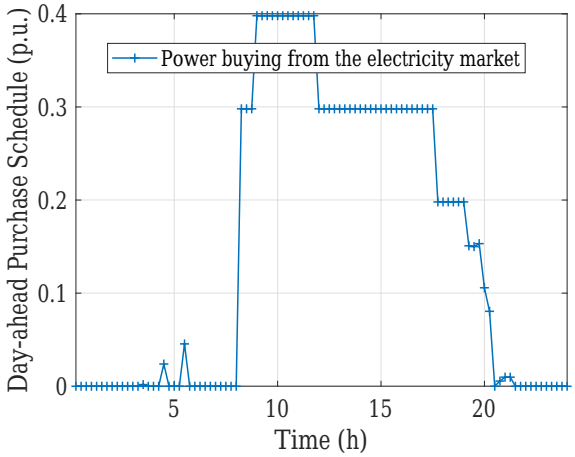

Fig. 5. The electricity buying from the day-ahead retail electricity market.

is tested with the 30 scenarios that were reduced from the original $1,000,000$ scenarios. The proposed two-stage risk-constrained stochastic programming approach is tested with the risk-aversion parameter $\kappa \in [0, 2]$ and the confidence level $\epsilon \in [0.89, 0.99]$. The large-scale MILP problem takes 1050 seconds to converge for each pair of risk-aversion parameters, e.g., $\kappa = 0.6, \epsilon = 0.99$, based on the 30 scenarios. As shown in the Fig. 2 and Fig. 3, for the two sets of confidence levels of 89% and 99%, by increasing the risk-aversion parameter κ from zero to two, the value of CVaR decreases and the expected O&M costs increase. The reason is that, with an increase in the risk-aversion parameter, the weighting related to the risk in the objective function also increases. Therefore, the first-stage decision variables and second-stage decision variables will work together to lower the CVaR by relying more on the expensive CHP units and reducing the electricity exchange with the main grid in case of islanding issues. This will result in an increase in the expected O&M costs of the commercial campus.

In order to select the proper risk-aversion parameter for further sensitivity analysis, based on the simulation results, we choose the $\kappa = 0.2$ and $\epsilon = 0.89$ as the risk-aversion parameter and the confidence level. This is because for the confidence level of 0.99, the decrement of CVaR is rather small at the beginning when compared with the one for 0.89 confidence level. Additionally, with the increase of risk-aversion parameter for $\epsilon = 0.89$, the CVaR deceases significantly at the beginning, which has the second lowest expected O&M costs at the point with $kappa = 0.2$.

2) First-Stage Decision Variables: The simulation results for the first-stage decisions based on the 30 scenarios with the $\kappa = 0.2$ and $\epsilon = 0.89$ are provided in Fig. 4, Fig. 5, and Fig. 6. As shown in Fig. 4, the CHP #1 is on during the entire operating day, where CHP #2 and CHP #3 are on during part of the business hours. This is because the generation costs and minimum up costs of the CHP #1 are less expensive than that of the CHP #2 and the CHP #3. Additionally, the day-ahead electricity buying/selling amount is based on the total islanding capability reserve.

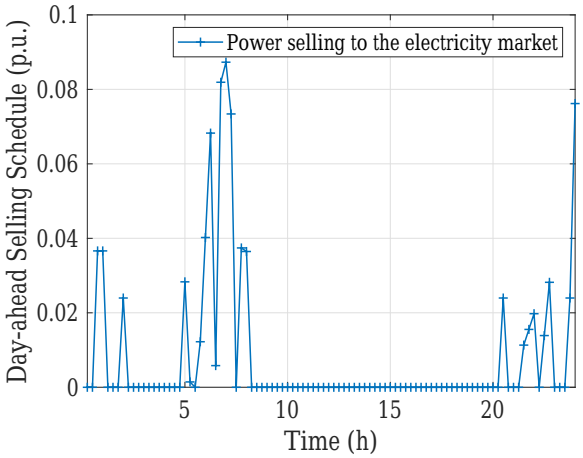

Fig. 6. The electricity selling to the day-ahead retail electricity market.

3) Islanding Capability with/without Reserves: The innovative contribution of this paper is use of an islanding capability based reserve method as a fundamental strategy for optimal energy management. We compare the proposed optimal energy management strategy with and without using the islanding capability based reserve method in the same uncertain grid-connection situation, where all other system settings remain the same. The islanding issue is set to occur at the 44-th time slot, where no power can be exchanged through the PCC at that time.

As shown in the Fig. 7, the reserve for buying/selling power from/to the retail electricity market is provided by three major components in the commercial campus: CHP units, ES units, and EWHs. The total selling reserve is provided by the ramping-down reserve from CHP units, the ramping-down reserve from ES units, and the ramping-down reserve from EWHs, respectively. The total buying reserve is provided by the ramping-up reserve from CHP units, and the ramping-up reserve from ES units. The islanding occurs at the 44-th time slot in the business hour, where the real-time power buying/selling from/to the retail electricity market is

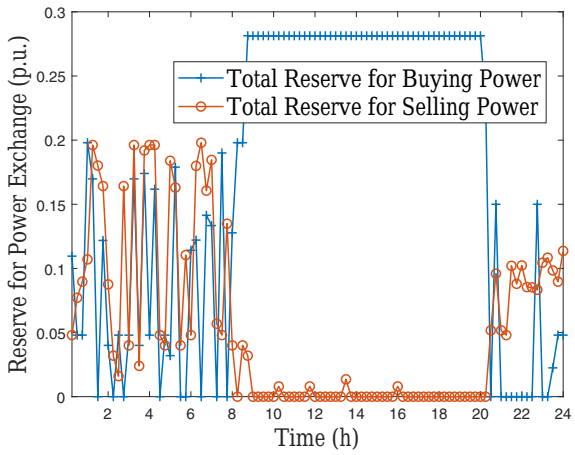

Fig. 7. The reserve for power exchange with the retail electricity market.

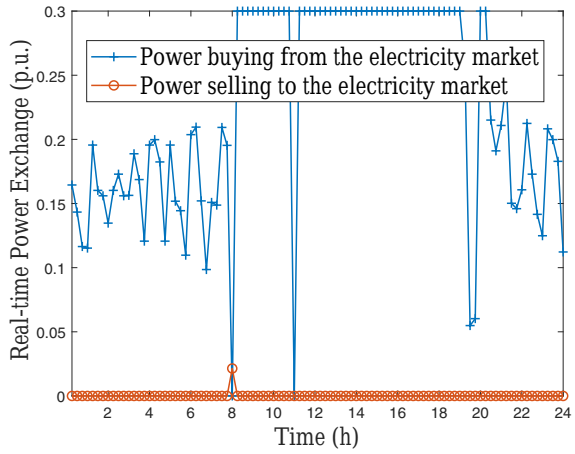

Fig. 8. The power exchange with the real-time retail electricity market when an islanding issue occurs in the operating day.

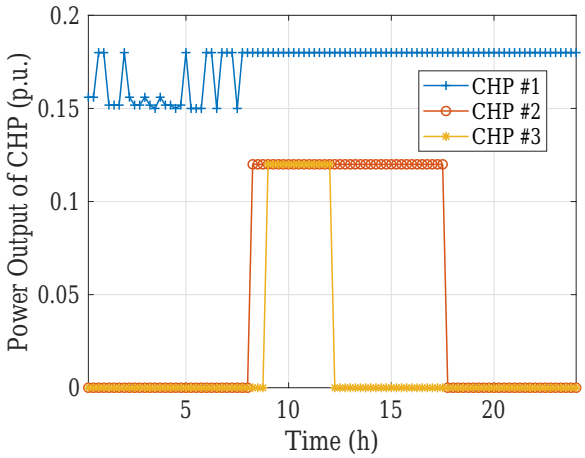

Fig. 9. The power output of CHP units when an islanding issue occurs in the operating day.

TABLE I
OPERATION AND MAINTENANCE COSTS

	With Reserve	Without Reserve
Costs ($)	17.34	31.57

zero in that time slot as shown in Fig. 8. During the islanding period, the shorted power is supported by CHP units and ES units, which increase the O&M costs only slightly but enhances the reliability of the commercial campus, which is demonstrated in Fig. 9. As shown in Fig. 4, CHP #1 is on during the entire operating day, where CHP #2 and CHP #3 are on during part of the business hours. This is because the generation costs and minimum up costs of CHP #1 are less expensive than that of CHP #2 and CHP #3.

The energy management strategy without islanding capability based reserve also relies on the ramping-up/ramping down capabilities of CHP units to survive through the period. However, the costs increased significantly from $17.34 to $31.57 (based on per unit values) as shown in Table I. This is reasonable since the power generated from CHP units is much more expensive than the reserved power from the ES units. Therefore, with the proposed reserve method, the reliability of the commercial campus can be maintained when an islanding issue occurs with lower O&M costs than that of the one without the proposed reserve method.

V. CONCLUSION

This paper proposes an optimal energy management strategy for campus-based commercial buildings with islanding capabilities to minimize total operation and maintenance costs, while maximizing comprehensive comfort levels for occupants. A two-stage scenario-based stochastic optimization approach is developed to handle various uncertainties associated with the energy management process, such as power generation of rooftop solar panels, arrival state-of-charges and arrival/departure time of plug-in electric vehicles, intermittent load demand in the commercial buildings, and uncertain grid-connection conditions. A conditional-value-at-risk method is adopted to provide a risk-averse energy management strategy. A scenario reduction method is leveraged to reduce the computational burden while maintaining the accuracy of the stochastic programming above a reasonable threshold. Extensive simulation results validate the effectiveness of the proposed optimal energy management strategy in minimizing the total operating and maintenance costs of commercial buildings with islanding capabilities, while maximizing the comprehensive comfort levels of the occupants.

REFERENCES

[1] L. Klein, J.-y. Kwak, G. Kavulya, F. Jazizadeh, B. Becerik-Gerber, P. Varakantham, and M. Tambe, "Coordinating occupant behavior for building energy and comfort management using multi-agent systems," *Automation in construction*, vol. 22, pp. 525–536, 2012.

[2] Z. Liang, Q. Alsafasfeh, T. Jin, H. Pourbabak, and W. Su, "Risk-constrained optimal energy management for virtual power plants considering correlated demand response," *IEEE Transactions on Smart Grid*, vol. 10, no. 2, pp. 1577–1587, 2017.

[3] C. D. Korkas, S. Baldi, I. Michailidis, and E. B. Kosmatopoulos, "Occupancy-based demand response and thermal comfort optimization in microgrids with renewable energy sources and energy storage," *Applied Energy*, vol. 163, pp. 93–104, 2016.

[4] Q. Zhou, Z. Li, Q. Wu, and M. Shahidehpour, "Two-stage load shedding for secondary control in hierarchical operation of islanded microgrids," *IEEE Transactions on Smart Grid*, vol. 10, no. 3, pp. 3103–3111, 2018.

[5] D. T. Nguyen and L. B. Le, "Joint optimization of electric vehicle and home energy scheduling considering user comfort preference," *IEEE Transactions on Smart Grid*, vol. 5, no. 1, pp. 188–199, 2014.

[6] Z. Liang, D. Bian, X. Zhang, D. Shi, R. Diao, and Z. Wang, "Optimal energy management for commercial buildings considering comprehensive comfort levels in a retail electricity market," *Applied Energy*, vol. 236, pp. 916–926, 2019.

[7] F. Chang, T. Chen, W. Su, and Q. Alsafasfeh, "Charging control of an electric vehicle battery based on reinforcement learning," in *2019 10th International Renewable Energy Congress (IREC)*, March 2019, pp. 1–63.

[8] J. Duan, K. Zhang, and L. Cheng, "A novel method of fault location for single-phase microgrids," *IEEE Transactions on Smart Grid*, vol. 7, no. 2, pp. 915–925, 2015.

[9] Z. Liang, A. Kavousifard, and W. Su, "Resilient restoration for distribution system operators when facing extreme events," in *2018 North American Power Symposium (NAPS)*. IEEE, 2018, pp. 1–6.

[10] A. Khodaei, "Microgrid optimal scheduling with multi-period islanding constraints," *IEEE Transactions on Power Systems*, vol. 29, no. 3, pp. 1383–1392, 2013.

[11] G. Liu, M. Starke, B. Xiao, X. Zhang, and K. Tomsovic, "Microgrid optimal scheduling with chance-constrained islanding capability," *Electric Power Systems Research*, vol. 145, pp. 197–206, 2017.

[12] X. Cao, J. Wang, J. Wang, and B. Zeng, "A risk-averse conic model for networked microgrids planning with reconfiguration and reorganizations," *IEEE Transactions on Smart Grid*, vol. 11, no. 1, pp. 696–709, 2019.

[13] V. Bui, A. Hussain, H. Kim, and Y. Im, "Optimal energy management of building microgrid networks in islanded mode considering adjustable power and component outages," *Energies*, vol. 11, no. 9, p. 2351, 2018.

[14] J. Liu, X. Cao, Z. Xu, X. Guan, X. Dong, and C. Wang, "Resilient operation of multi-energy industrial park based on integrated hydrogen-electricity-heat microgrids," *International Journal of Hydrogen Energy*, 2021.

[15] S. Acharya, M. El-Moursi, A. Al-Hinai, A. Al-Sumaiti, and H. Zeineldin, "A control strategy for voltage unbalance mitigation in an islanded microgrid considering demand side management capability," *IEEE Transactions on Smart Grid*, vol. 10, no. 3, pp. 2558–2568, 2018.

[16] Z. Li and Y. Xu, "Optimal coordinated energy dispatch of a multi-energy microgrid in grid-connected and islanded modes," *Applied Energy*, vol. 210, pp. 974–986, 2018.

[17] J. Duan, H. Xu, W. Liu, J. Peng, and H. Jiang, "Zero-sum game based cooperative control for onboard pulsed power load accommodation," *IEEE Transactions on Industrial Informatics*, 2019.

[18] R. Fernández-Blanco, Y. Dvorkin, B. Xu, Y. Wang, and D. S. Kirschen, "Optimal energy storage siting and sizing: A wecc case study," *IEEE Transactions on Sustainable Energy*, vol. 8, no. 2, pp. 733–743, 2016.

[19] J. Duan, Z. Yi, D. Shi, C. Lin, X. Lu, and Z. Wang, "Reinforcement-learning-based optimal control for hybrid energy storage systems in hybrid ac/dc microgrids," *IEEE Transactions on Industrial Informatics*, 2019.

[20] M. A. Bagherian and K. Mehranzamir, "A comprehensive review on renewable energy integration for combined heat and power production," *Energy Conversion and Management*, vol. 224, p. 113454, 2020.

[21] Y. Zong, D. Kullmann, A. Thavlov, O. Gehrke, and H. W. Bindner, "Application of model predictive control for active load management in a distributed power system with high wind penetration," *IEEE Transactions on Smart Grid*, vol. 3, no. 2, pp. 1055–1062, 2012.

[22] Y. Lin and Z. Bie, "Tri-level optimal hardening plan for a resilient distribution system considering reconfiguration and dg islanding," *Applied Energy*, vol. 210, pp. 1266–1279, 2018.

[23] E. Cesena, N. Good, A. Syrri, and P. Mancarella, "Techno-economic and business case assessment of multi-energy microgrids with co-optimization of energy, reserve and reliability services," *Applied Energy*, vol. 210, pp. 896–913, 2018.

[24] X. Cao, T. Cao, F. Gao, and X. Guan, "Risk-averse storage planning for improving res hosting capacity under uncertain siting choice," *IEEE Transactions on Sustainable Energy*, 2021.

[25] R. T. Rockafellar and S. Uryasev, "Optimization of conditional value-at-risk," *Journal of risk*, vol. 2, pp. 21–42, 2000.

[26] Y. Wang, Y. Liu, and D. S. Kirschen, "Scenario reduction with submodular optimization," *IEEE Transactions on Power Systems*, vol. 32, no. 3, pp. 2479–2480, 2017.

[27] Z. Liang and Y. Guo, "Optimal energy management for microgrids with cogeneration and renewable energy sources," in *Smart Grid Communications (SmartGridComm), 2015 IEEE International Conference on*. IEEE, 2015, pp. 647–652.

[28] "National Wind Technology Center M2 Tower," http://www.nrel.gov/midc/nwtc_m2/, 2019, last retrieved in July 3, 2019.

[29] "PJM Day-ahead and Real-Time Electricity Prices," http://www.pjm.com/markets-and-operations.aspx, 2019, last retrieved in July 3, 2019.